

THE PENNSYLVANIA STATE UNIVERSITY
SCHREYER HONORS COLLEGE

DEPARTMENT OF CHEMICAL ENGINEERING

OPTICAL PROPERTIES OF CONJUGATED POLYMERS IN SOLUTION

CURTIS SILVERIA
FALL 2017

A thesis
submitted in partial fulfillment
of the requirements
for a baccalaureate degree in Chemical Engineering
with honors in Chemical Engineering

Reviewed and approved* by the following:

Dr. Enrique Gomez
Associate Professor of Chemical Engineering
Thesis Supervisor

Dr. Michael Janik
Professor of Chemical Engineering
Honors Adviser

* Signatures are on file in the Schreyer Honors College.

ABSTRACT

Control of optical properties of conjugated polymers can be critical for conversion efficiency of plastic solar cells. In pure polymer and solvent systems, solvent effects on the optical properties of the dissolved polymer could provide information to optimize performance in a full device. The absorbance spectra and photoluminescence spectra of poly(3-hexylthiophene), Poly[N-9'-heptadecanyl-2,7-carbazole-alt-5,5-(4',7'-di-2-thienyl-2',1',3'-benzothiadiazole)], and poly(2,7-(9',9'-dioctylfluorene)-alt-5,5-(4',7'-di-2-thienyl-2',1',3'-benzothiadiazole) in dilute solutions with organic solvents were studied and an increase in band gap energy with increasing solvent refractive index was observed. Dilute solutions allowed trends to be linked to free-floating chains, eliminating microstructure formation.

TABLE OF CONTENTS

LIST OF FIGURES iii

ACKNOWLEDGEMENTS iv

Chapter 1 Introduction 1

Chapter 2 Experimental Methods 5

Chapter 3 Experimental Results and Discussion 6

Chapter 4 Conclusion and Future Work 14

BIBLIOGRAPHY 15

LIST OF FIGURES

- Figure 1. Diagram showing the beginning process of electricity generation system in an organic solar cell with p-type donor P3HT and n-type acceptor PCBM. The major steps, excitation, dissociation, and charge separation are visualized.....2
- Figure 2. (a) UV absorbance spectra of PCDTBT with the absorption peak of the π - π^* transition of the main chains at 395nm and the intramolecular charge transfer peak (ICT) noted at 561nm. (b) A representation of the electron donating and accepting regions of the PCDTBT subunits4
- Figure 3. Normalized UV-vis spectra of P3HT in different common organic solvents.....6
- Figure 4. (a) Critical wavelength of P3HT based on the refractive index of different organic solvents (b) Critical wavelength of P3HT based on molecular volume of the solvent. ...7
- Figure 5. (a) Emission spectra of P3HT in different organic solvents at an excitation wavelength of 470nm. (b) The peak wavelength of the emission spectra of P3HT in each organic solvent based on refractive index. (c) The peak wavelength of the emission spectra8
- Figure 6. Normalized absorbance spectra of PCDTBT at 0.003mg/ml in various solvent systems.9
- Figure 7. (a) Main chain π - π^* transition peak of PCDTBT in each solvent based on molecular volume. (b) Main chain π - π^* transition peak of PCDTBT based on refractive index. (c) Intramolecular charge transfer peak based on molecular volume. (d) Intramolecular charge transfer peak shift based on refractive index of the solvent.10
- Figure 8. (a) Emission spectra of PCDTBT in organic solvents, excitation at 370nm. (b) Emission maxima wavelength vs refractive index of solvent. (c) Emission maxima wavelength vs molecular volume of solvent..... 11
- Figure 9. Normalized absorbance spectra of PFT6BT at 0.003mg/ml in various solvents.....12
- Figure 10. (a) Peak wavelength of PFT6BT main chain π - π^* transition based on molecular volume of the solvent. (b) Peak wavelength of PFT6BT main chain π - π^* transition based on refractive index of the solvent. (c) PFT6BT ICT peak wavelength based on solvent molecular volume. (d) PFT6BT ICT peak wavelength based on the solvent refractive index.13

ACKNOWLEDGEMENTS

I would like to thank Dr. Enrique Gomez and Melissa Aplan for their guidance and instruction on this project. Without their help, this project would have not been possible. Thanks are also owed to Dr. Janik who has done a great job as an advisor.

Chapter 1

Introduction

Renewable energy sources are seeing increasing growth as the world energy demand increases and viable fossil fuel alternatives become more dependable. A promising energy source has been solar power, harnessing the light energy from sunlight and converting it into electricity directly via a photovoltaic solar cell. A major drawback to the current technology of traditional silicon base solar cells is the high expense of manufacturing leading to high capital costs. The solar cells are very rigid and heavy due to the large amount of silicon used in their manufacturing. Low capital cost and weight limited applications struggle to work with current technologies, but polymer based organic solar cells have the potential to provide a cheap and lightweight alternative¹.

Flexible polymer base photovoltaic devices, also known as organic photovoltaic devices, offer a unique set of benefits and drawbacks from traditional silicon based devices. Using semiconducting polymers enables thin product layers to be applied on the device, allowing extremely light and flexible devices to be made at a fraction of the cost. In production, organic solar cells are capable of being produced in high-throughput, roll-to-roll processing, similar to newspaper, greatly reducing the capital cost of the product².

The overall design of an organic solar cell is rather similar to a traditional battery, attempting to maximize the photo electric effect. The device utilizes two metal electrodes and an electrolyte rich medium to facilitate charge transport and form a direct current. The main change is the electrolyte in the organic solar cell is now a polymer-based medium that enables ion exchange while

converting light into usable energy. The conversion process consists of excitation, dissociation, charge separations, and finally conduction between the electrodes.

The important photoactive polymers used in organic solar cells have delocalized π electrons and are capable of absorbing sunlight. The polymers can generate charges as the sunlight excites the delocalized electrons and transport the charges through the device or system. A brief diagram of how the charge generation and transport occurs can be seen in figure 1.

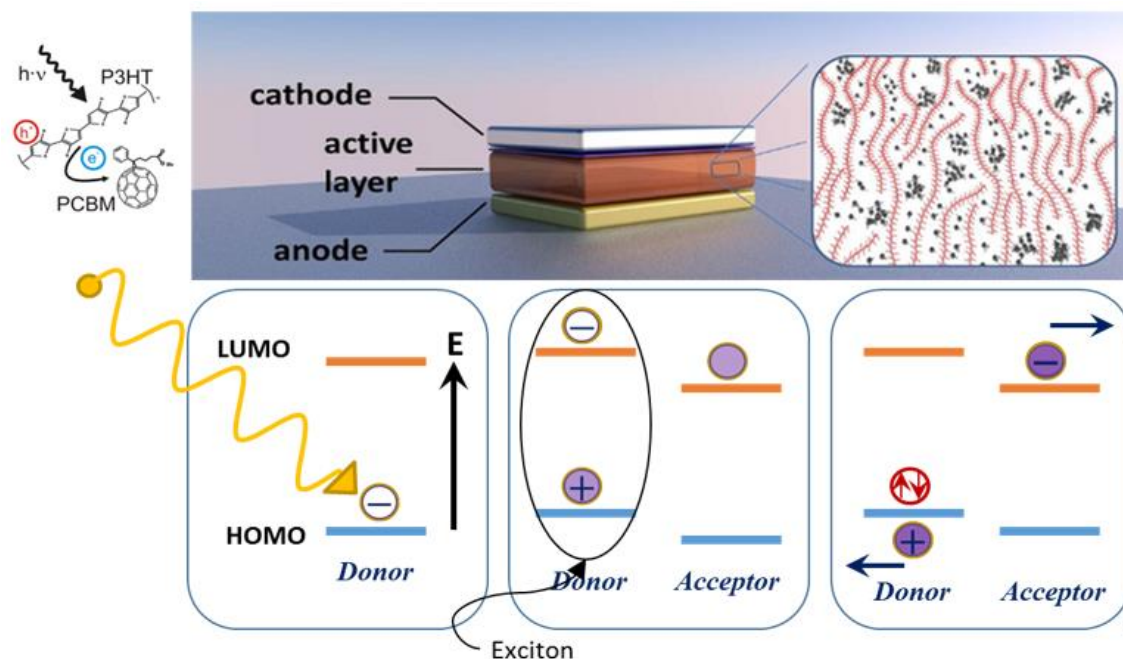


Figure 1. Diagram showing the beginning process of electricity generation system in an organic solar cell with p-type donor P3HT and n-type acceptor PCBM. The major steps, excitation, dissociation, and charge separation are visualized.

In figure 1 the first three steps of the energy generation process are described. The sunlight photon hits the p-type or electron donating polymer in the system. The p-type polymer, in this case P3HT, can have an electron excited from the highest occupied molecular orbital (HOMO) to the lowest unoccupied orbital (LUMO). The difference in energy of these two orbitals is the minimum amount of energy required from the photon to successfully excite the electron. The initial excited state

consist of the negatively charge electron in the LUMO and a positive charge in the hole left behind in the HOMO and is collectively called an exciton. The energy difference of the HOMO and LUMO can be described as the band-gap energy E_g . The exciton now can either collapse on itself, losing all the energy potential created, or find an interface between the p-type polymer and n-type polymer where the exciton can dissociate, allowing the electron to migrate to the cathode and the hole to migrate to the anode of the device. Electricity is then generated from the flowing of electrons³.

In all semiconductors, including polymer based, there is a cutoff wavelength where the absorption characteristics of the material become negligible, known as the critical wavelength. The critical wavelength (λ_c) is related to the band-gap energy E_g by the relation $E_g = hc / \lambda_c$. In UV-vis spectroscopy, the onset of absorption is typically used as the critical wavelength of the material. For materials with near identical absorption spectra shapes, changes in maxima of absorbance indicates a change in the onset of absorption. The band-gap energy within semi-conductors is determined by the π - π^* transition energy of the conjugated main chains for each polymer as well as the intramolecular charge transfer (ICT) interactions exhibited in both PCDTBT and PFT6BT. A visualization of this phenomena for PCDTBT can be seen in figure 2 and is similar to the interactions within PFT6Bt subunits. P3HT spectra only contains the conjugated main chain transition due to the lack of an electron accepting region within the subunit⁴.

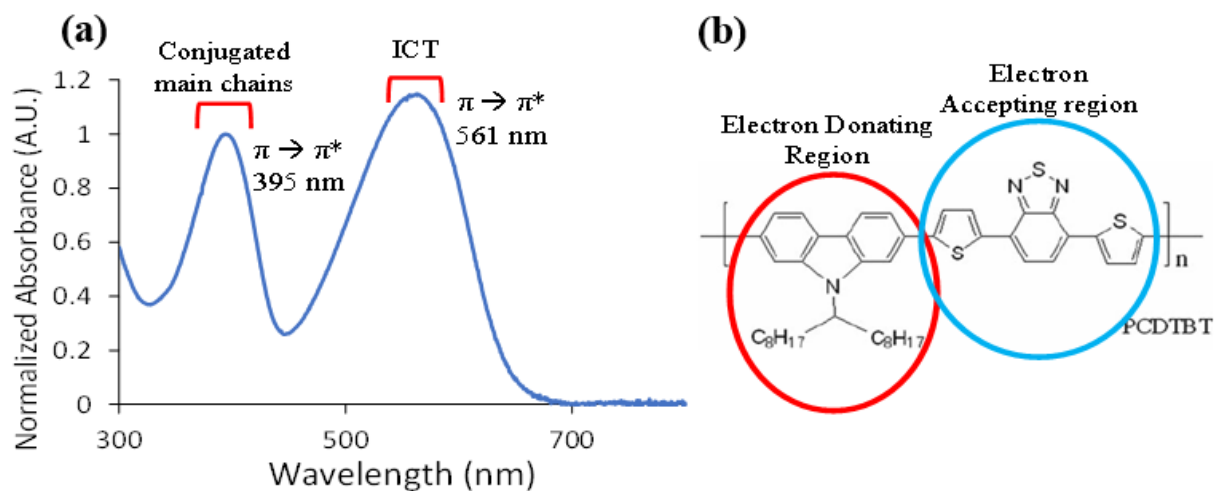


Figure 2. (a) UV absorbance spectra of PCDTBT with the absorption peak of the π - π^* transition of the main chains at 395nm and the intramolecular charge transfer peak (ICT) noted at 561nm. (b) A representation of the electron donating and accepting regions of the PCDTBT subunits

Little is known about how the solvents used in making organic solar cell devices may affect the band-gap energy of the polymer. In the following experiment, 4 major organic solvents are used to dissolve P3HT, PCDTBT, and PFT6BT. Through UV-spectroscopy, critical factors controlling λ_c and thus E_g could be identified and photoluminescence spectroscopy provided a means of confirming observed trends for P3HT and PCDTBT⁵.

Chapter 2

Experimental Methods

Sample Preparation

All polymers were dissolved in anhydrous chlorobenzene, 1,2-dichlorobenzene, 1,2,4-trichlorobenzene, and chloroform (Sigma-Aldrich) at 0.15 mg/ml in a nitrogen-filled glovebox and stirred overnight at 40-50C. Before measurements, the samples were diluted to 0.03mg/ml and loaded into quartz cuvettes (1 cm path length), and sealed. Once removed from the glovebox, measurements were taken within an hour.

Absorbance and Photoluminescence Spectroscopy

For polymer solutions, absorbance spectra were measured using a UV-vis spectrometer (Agilent Technologies, Cary60). Photoluminescence spectra were collected using a spectrofluorometer (Photon Technology International) with an excitation wavelength of 470 nm (P3HT), 370 nm (PCDTBT) and a spectral resolution was 2 nm.

Chapter 3

Experimental Results and Discussion

Figure 3a compares the ultraviolet-visible (UV-visible) absorption spectra of P3HT in different organic solvents at dilute solutions. P3HT had similar absorption spectrum shape for each organic solvent tested, but an absorption maxima shift can be seen from 450-475nm. The absorption spectra is attributable to the π - π^* transition energy of P3HT's conjugated main chains. The critical wavelength was 443nm, 456nm, 462nm, and 473nm for chloroform, chlorobenzene, 1,4-dichlorobenzene and 1,2,4-trichlorobenzene respectively. It was theorized that the dielectric constant of the solvents would be directly influenced the critical wavelength of P3HT. However, the results of this initial experiment lead to the conclusion that the solvent dielectric constant had little to do with change seen in the critical wavelength. Refractive index of the solvents did seem to hold a linear trend with the shift observed seen in figure 4a.

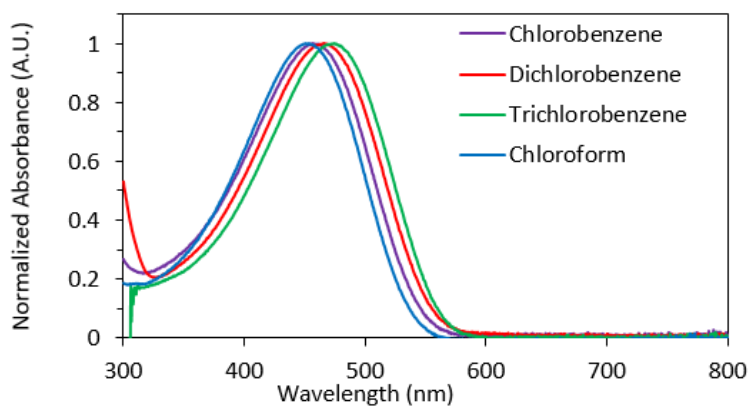


Figure 3. Normalized UV-vis spectra of P3HT in different common organic solvents.

One possible explanation for the observed redshift of P3HT is the refractive index change of the solvent. In figure 4a the trend between the critical wavelength and the refractive index of the solvent looks linear. It is possible that the solvent can either change the orientation of the P3HT molecule or change the energy levels of the π and or π^* states, resulting in a change of the band-gap energy of P3HT. In figure 4b, molecular volume of the solvent could also play a role in the observed red shift of P3HT as a very similar trend can be seen in figure 4a as seen with refractive index. The reasoning behind how the molecular volume would affect the band-gap energy of P3HT is a bit harder to explain however.

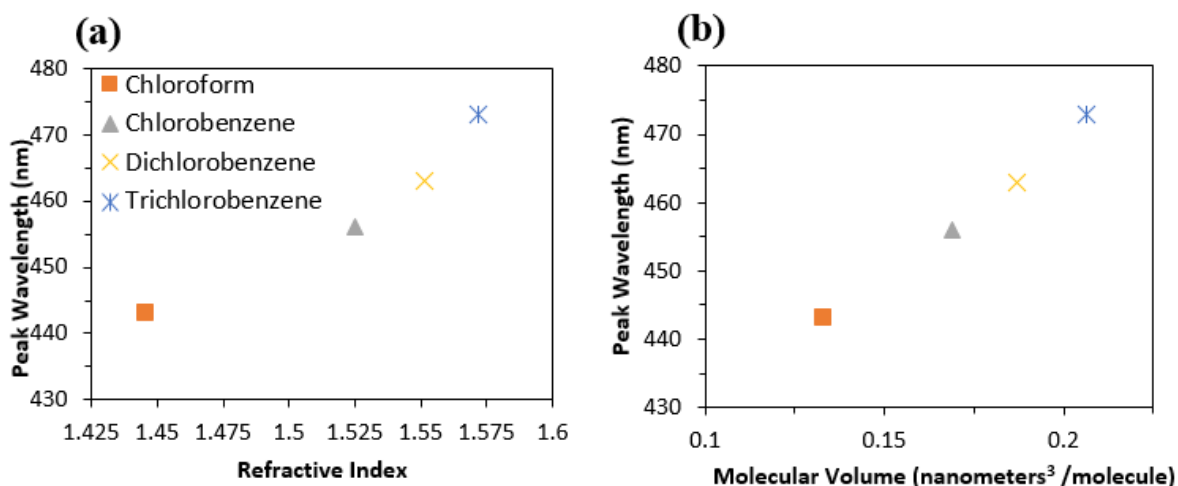


Figure 4. (a) Critical wavelength of P3HT based on the refractive index of different organic solvents (b) Critical wavelength of P3HT based on molecular volume of the solvent.

To confirm the UV-vis results photoluminescence spectroscopy was performed on P3HT in each solvent. The emission spectra seen in figure 5a shows an emission peak between 575-588nm depending on the organic solvent used. Figure 5b shows a redshift as refractive index of the solvent increases, confirming the trend seen in the UV-vis data.

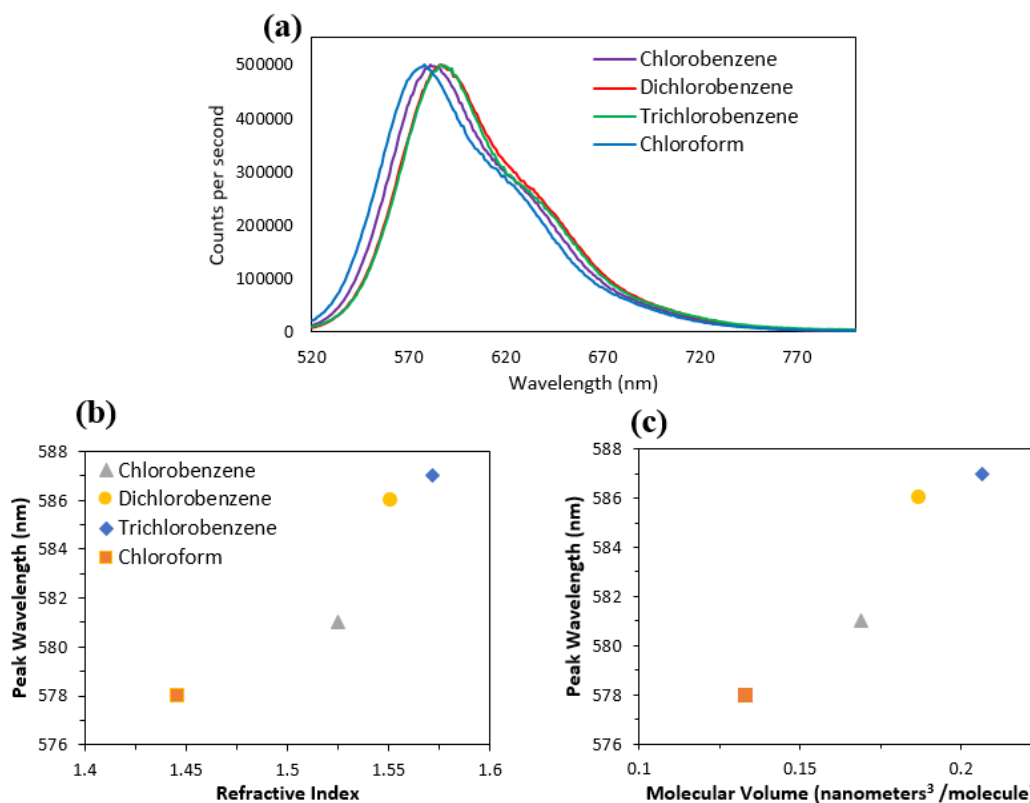


Figure 5. (a) Emission spectra of P3HT in different organic solvents at an excitation wavelength of 470nm. (b) The peak wavelength of the emission spectra of P3HT in each organic solvent based on refractive index. (c) The peak wavelength of the emission spectra

Seen in figure 6, PCDTBT contains two absorbance spectra maxima at around 395nm and 564nm.

The UV-visible absorbance spectra of PCDTBT indicated a redshift of both the conjugated main chain π - π^* transition seen in the 395nm region and the intramolecular charge transfer peak at around 564nm. The redshift trends are like those seen with P3HT, however, the chloroform peak falls far out of the trend. The chloroform peak is at a higher wavelength than the chlorobenzene sample, indicating the previous conveyed trend may only apply to the P3HT polymer.

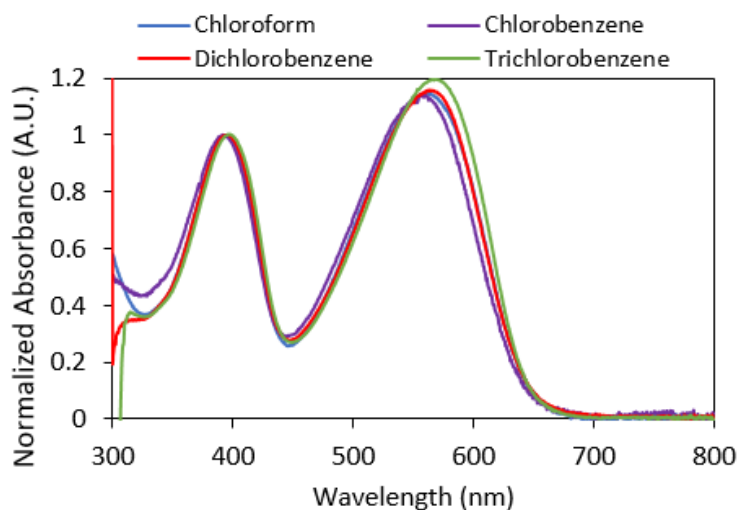


Figure 6. Normalized absorbance spectra of PCDTBT at 0.003mg/ml in various solvent systems.

In figure 7a trend can be seen with both the refractive index and the molecular volume of the solvent for the chlorinated benzene solvents, indicating that one or both aspects can influence the band gap energy of the polymer. Interestingly the intramolecular charge transfer maxima experience a larger redshift than the main chain peak for the chlorinated benzene solvents. It seems the band gap energy of the lower energy charge transfer between the carbazole moieties and benzothiadiazole moieties more sensitive to the solvent environment than the π - π^* transition state⁷.

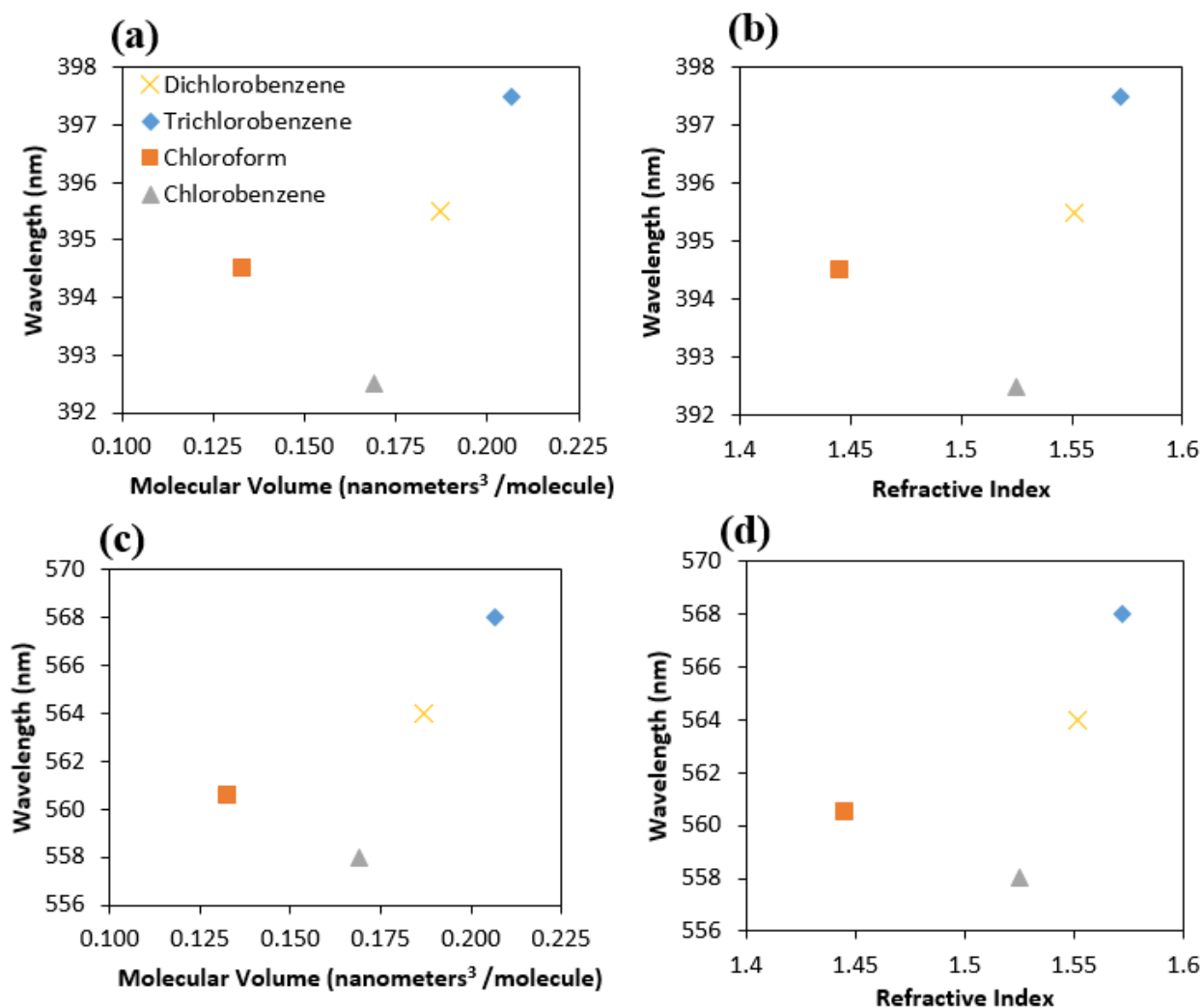


Figure 7. (a) Main chain π - π^* transition peak of PCDTBT in each solvent based on molecular volume. (b) Main chain π - π^* transition peak of PCDTBT based on refractive index. (c) Intramolecular charge transfer peak based on molecular volume. (d) Intramolecular charge transfer peak shift based on refractive index of the solvent.

Photoluminescence spectroscopy emission spectra of PCDTBT in figure 8a did not replicate a similar redshift trend for chlorinated benzene solvents for the π - π^* transition state peak. The emission maxima based on molecular volume and refractive index seen in figure 8b and figure 8c respectively did not indicate any trend. The structure of PCDTBT is very different from that of P3HT and is slightly less soluble. Incomplete dissolution could cause changes in observed trends. Concentration also effects the emission spectra peak and differences in relative concentrations influence the general trends observed.

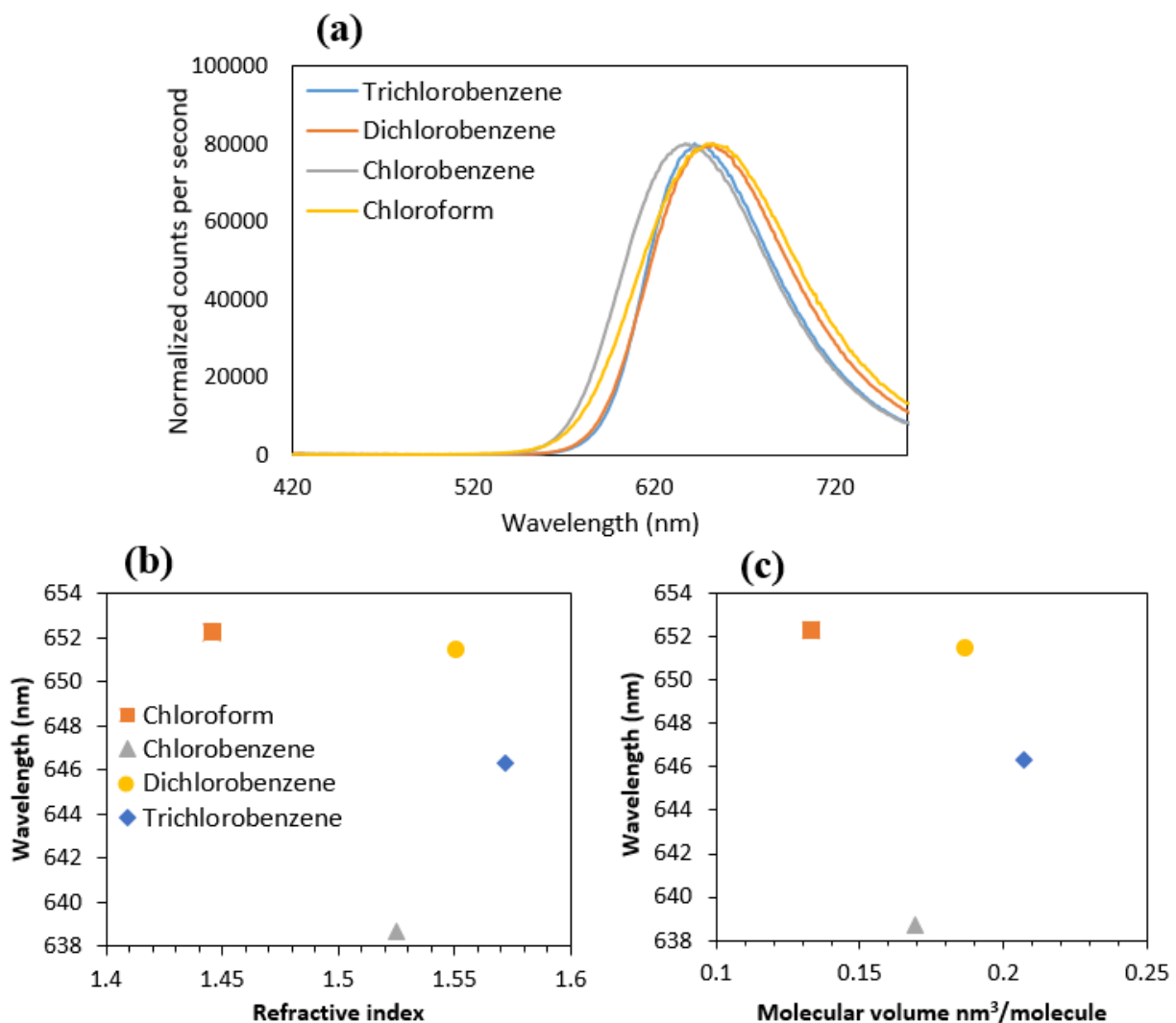


Figure 8. (a) Emission spectra of PCDTBT in organic solvents, excitation at 370nm. (b) Emission maxima wavelength vs refractive index of solvent. (c) Emission maxima wavelength vs molecular volume of solvent.

Figure 9 compares the UV-visible spectrum of PFT6BT in multiple organic solvents. Absorption maxima can be seen around 367nm and 520nm. Like PCDTBT, the first peak around 367nm represents the main chain π - π^* transition energy peak and the peak around 520nm represents the ICT within the sub units.

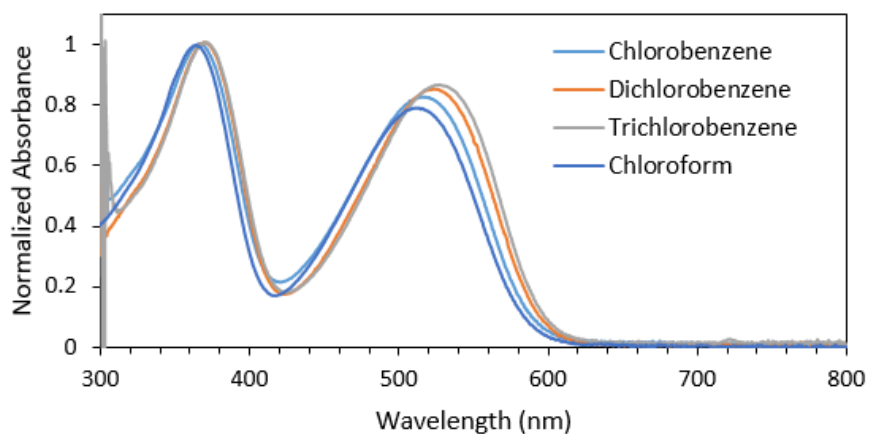


Figure 9. Normalized absorbance spectra of PFT6BT at 0.003mg/ml in various solvents.

Figure 10 shows a trend that there is a redshift of the absorption maxima for both the main chain peak and the ICT peak for PFT6BT. The ICT maxima peak at 520nm experiences a stronger redshift than the main chain peak at 367nm. The redshift trends of PFT6BT follow that of PCDTBT. The solvent can influence the band-gap energy from its ability to stabilize two-point charges. The ICT interactions seem to be influenced more by the phenomena. Unlike the PDCTBT trial, chloroform followed the same trend as the chlorinated benzenes. PFT6BT is readily more soluble than PCDTBT and is likely that the better solubility in chloroform led to the continuation of the redshift trend.

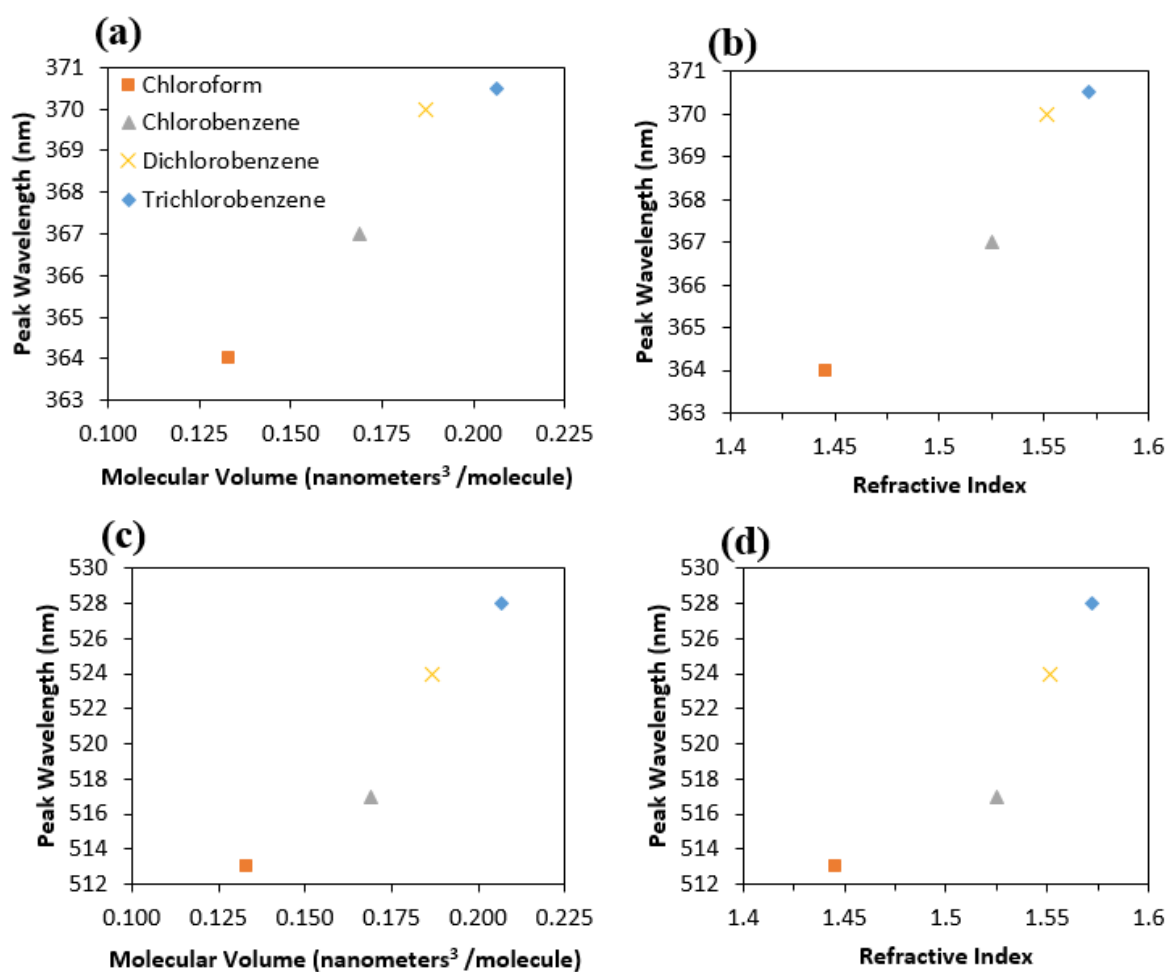


Figure 10. (a) Peak wavelength of PFT6BT main chain π - π^* transition based on molecular volume of the solvent. (b) Peak wavelength of PFT6BT main chain π - π^* transition based on refractive index of the solvent. (c) PFT6BT ICT peak wavelength based on solvent molecular volume. (d) PFT6BT ICT peak wavelength based on the solvent refractive index.

Chapter 4

Conclusion and Future Work

Conclusion

Conjugated polymers P3HT, PCDTBT, and PFT6BT, all show a critical wavelength and thus band gap energy response to the solvent environment. Free floating chains of the polymers at dilute concentrations show trends of a redshift or reducing the overall band gap energy of the π - π^* transition as refractive index increases. Molecular volume may also play a role, though explanation of how this would affect the energy band gap is harder to explain. Photoluminescence spectroscopy emission scans confirmed the observed trend for P3HT but was unable to confirm the trend for PCDTBT. The intramolecular charge transfer for the PCDTBT and PFT6BT polymers experienced a larger redshift, indicating the phenomena is pronounced in the charge transfer within subunits. In device design it may be important to consider how solvent selection can alter characteristics of the working electron donor polymers.

Future Work

Future investigations include determining if aggregation could influence the trends observed in this study. Performing dynamic light scattering of samples of slightly higher concentration could determine the average size of the dissolved polymers and determine if aggregates are present. Investigation of other solvents that have a refractive index and molecular volume very different to the previously studied solvents could help determine which solvent characteristic causes changes in band gap energy. Solubilizing the polymers effectively will be required as well.

BIBLIOGRAPHY

- [1] Singh, R. P.; Kushwaha, O. S. *Macromolecular Symposia* **2013**, 327 (1), 128–149.
- [2] Pivrikas, A. *Solar Cells - New Aspects and Solutions* **2011**.
- [3] Mahakul, P. C.; Sa, K.; Das, B.; Mahanandia, P. *Materials Chemistry and Physics* **2017**, 199, 477–484.
- [4] Dailing, E. A.; Nair, D. P.; Veer, T. V. D.; Dovidio, T.; Stansbury, J. W. *Macromolecular Chemistry and Physics* **2017**, 218 (21), 1700256.
- [5] Kleinhenz, N.; Rosu, C.; Chatterjee, S.; Chang, M.; Nayani, K.; Xue, Z.; Kim, E.; Middlebrooks, J.; Russo, P. S.; Park, J. O.; Srinivasarao, M.; Reichmanis, E. *Chemistry of Materials* **2015**, 27(7), 2687–2694.
- [6] Hawks, S. A.; Aguirre, J. C.; Schelhas, L. T.; Thompson, R. J.; Huber, R. C.; Ferreira, A. S.; Zhang, G.; Herzing, A. A.; Tolbert, S. H.; Schwartz, B. J. *The Journal of Physical Chemistry C* **2014**, 118(31), 17413–17425.
- [7] Duan, C.; Cai, W.; Hsu, B. B. Y.; Zhong, C.; Zhang, K.; Liu, C.; Hu, Z.; Huang, F.; Bazan, G. C.; Heeger, A. J.; Cao, Y. *Energy & Environmental Science* **2013**, 6(10), 3022.

ACADEMIC VITA
Academic Vita of Curtis Silveria
curtissilveria@gmail.com

Bachelor of Science in Chemical Engineering, Schreyer Honors College
Honors in Chemical Engineering.

Optical Properties of Conjugated Polymers in Solution
Thesis Supervisor: Assistant Professor of Chemical Engineering Dr. Gomez

EXPERIENCE

PepsiCo Gatorade Production Intern

July 2017- August 2017

Mountain Top PA

- Examined the Waste Water facility at a Union Gatorade production plant to determine root cause of bioreactor failure
- Performed DMAIC and Lean Six Sigma processes to determine best courses of action

Key Successes

- Formed multifunctional team to create robust procedures for future bioreactor health and efficacy
- Produced training documents, slide decks, and SOPs regarding Waste Treatment concerns

Johnson and Johnson Consumer R&D Co-op: Sunscreen Formulator

January 2016- August 2016

Skillman, NJ

- Formulation lead for a technology project for Global SunCare
- Developed SPF 30, 50, and 50+ formulations with high PFA Protection composed of inorganic, organic, and hybrid sunscreen actives

Key Successes

- Developed 4+ new Sunscreen Chassis including sunscreen sticks, lotions and sprays
- Utilized instruments including Rheometer, Dynamic Laser Light Scattering, Lab Sphere, Microscopy to measure rheological profiles, particle size, in vitro SPF assessments, and package compatibility
- Drove collaboration between Technology Formulation Team and Packaging Innovation
- Connected with Subject Matter Experts across Global Beauty Organization, aligning with suppliers to strengthen sunscreen technology at J&J consumer

RESEARCH

Penn State University Chemical Engineering Laboratory

September 2014- Present

State College, PA

- Trained and led 2 undergraduate researchers in the Gomez group
- Investigated 5 solvent environments and 2 polymer traits that could affect polymer performance in solar cell devices with spectroscopy techniques including Dynamic Light Scattering, UV-Vis, and Fluorescence spectroscopy
- Compiled data in Excel and utilized Solver to make accurate curve fits, presented summarized data weekly to discuss the projects next objectives